Longitudinal Trim and Stability Analysis of Generic Air-Breathing Hypersonic Vehicle using Bifurcation Method

Ritesh SINGH*,[1,2], Om PRAKASH[2], Sudhir JOSHI[2], Yogananda JEPPU[3]

*Corresponding author
*,[1]Department of Electrical Engineering, Manipal University Jaipur
Jaipur, Rajasthan, 303007, India
ritesh.singh23@gmail.com
[2]Department of Aerospace Engineering, University of Petroleum & Energy Studies,
Dehradun, Uttarakhand, 248007, India
omprakash@ddn.upes.ac.in, sjoshi@ddn.upes.ac.in
[3]Aerospace Electronics Solutions, Honeywell Technology Solutions,
Hyderabad, Telangana, 500032, India,
yvjeppu@gmail.com

DOI: 10.13111/2066-8201.2022.14.3.10

Received: 08 March 2022/ Accepted: 24 August 2022/ Published: September 2022

Abstract: *The Air-breathing Hypersonic Vehicle (AHV) can meet the futuristic goals of rapid global travel, to Low-Earth Orbit and into space in near-term decades. This paper presents the study of the trim and stability characteristics of the 3DOF longitudinal model of the generic AHV. Longitudinal 3DOF AHV simulation is developed with the aerodynamic model for trim analysis considering the complete flight envelope for Mach number from M=0 to 24. Dynamic model simulation of the 3DOF AHV is performed for the trim conditions and stability of the AHV flight for the complete envelope. Bifurcation Analysis is implemented with the longitudinal 3DOF AHV model for trim analysis and stability for the complete AHV flight envelope.*

Key Words: *Dynamic Simulation, 3DOF Longitudinal Model, Trim Analysis, Stability, Air-breathing Hypersonic Vehicle, AHV, Bifurcation Analysis*

1. INTRODUCTION

AHV can offer beneficial technology for routine space access at a low cost. It provides the way forward with a key function in space transportation and tourism. Hypersonic flight can provide low cost/ inexpensive access to LEO (Low Earth Orbit) for space missions and commercial applications. With NASA's program, decades of success and the need for a reliable and affordable space entrance for a variety of commercial and military purposes, the interest in hypersonic vehicles has been renewed. Single Stage To Orbit (SSTO) flights using AHV technology are on the horizon for a variety of military and commercial purposes, with huge potential for space tourism. All the common public, engineers, scientists and space lovers dream of flying in space. Hypersonic vehicles may prove to be an appropriate platform for the second-stage rocket and are capable of SSTO in the coming decades. Research into AHVs started in the 1960s and was persistent into the 1990s with the US hypersonic programs. The development of an operational AHV will involve the most important developments in

propulsion technology, multidisciplinary modeling and simulation, and design benchmarks/ milestones. On the development and research front of AHV, the focus is on the propulsion technology so that hypersonic flight and wide-range speed in different sonic and hypersonic regimes can be achieved. Thus, this propulsion system must maintain the low altitude flight in order to attain the high stagnation pressure for better engine performance. These analysis points are used in the simulations to produce initial conditions that are similar to those in flight. Using aircraft aerodynamic and propulsion system models, trim analysis can offer the necessary data to establish the operating envelope or performance characteristics of an aircraft. Trim points are often where linear models are created and trim conditions specify the points at which control systems are designed and evaluated. As a result, we can use these trim conditions as an initial point for comparisons between other models and it can be implemented differently based on the actual flight data. Trim analysis is used to minimize a cost function with constraints [1] for nonlinear aircraft models developed considering aerodynamic and propulsion models. It presents a trim algorithm that is implemented for the simulation of the 6DOF aircraft model. It presents a trim algorithm which is implemented for the simulation of the 6DOF aircraft model. Analysis of parafoil system using trim and stability from [2], uses bifurcation technique and discusses the impact of the model constraints on the longitudinal dynamics with trim along with stability traits for 4DOF longitudinal dynamic flight model. Analysis of trim conditions [3] for nonlinear flight control law development is carried out using a model-based control structure. It shows trimmed flight analysis using outer loop and inner loop equations in the 6DOF aircraft model for different control surface deflections. Trim analysis using equations of motion for aircraft design is presented for steady-state straight flight [4] and for turning, pull up and pull overflight [5]. The study is related to trimming the 6DOF conventional and unconventional aircraft for control power assessment and to formulate a generic analytical framework for trim analysis. The longitudinal flight dynamics play a vital role in the flight maneuvers as most of the flight duration corresponds to longitudinal flight dynamics in the longitudinal frame. Longitudinal flight includes the complete flight regime, comprising velocity in the fixed X and Z plane of the body, and level flight, climb and descent, and, pull-up and pull-down flight. This shows that longitudinal flight dynamics should be the major concern for the trim and stability analysis. This paper provides the trim analysis of the Generic AHV dynamic model and its stability analysis. It provides the trim simulation of the AHV for the complete flight envelope for Mach number from M=0 to 24, and its dynamic analysis using the Bifurcation Method considering the eigenvalues approach and longitudinal modes analysis of the AHV flight.

2. 3DOF LONGITUDINAL MODEL

The Winged Cone model is a GHV (Generic Hypersonic Vehicle) simulation model built by NASA Langley Research Centre [6], shown in Fig. 1, and is used for the analysis of the longitudinal model. The propulsion system is hypothetically proposed with a combination of turbojet, ramjet and scramjet, and the rocket propulsion system is incorporated into the model. The Center of mass, centre of gravity, and moments of inertia are included in the equations of motion of the generic 3DOF AHV model for simulation. The total mass of the vehicle, center of gravity location and products of inertia vary as fuel is consumed. The X-axis of the body is completely aligned with the orientation of the vehicle thrust vector. As a result, there is no thrust force component in the body's Y and/or Z-axis. Because to this, it is expected that when the fuel is spent, the center of gravity will only shift along the x-axis of the body. The AHV 3DOF model is modelled and simulated using the flat Earth approximation and equations of

motion are established using Newton's and Euler's equations. Table 1 shows the geometric specifications of the vehicle.

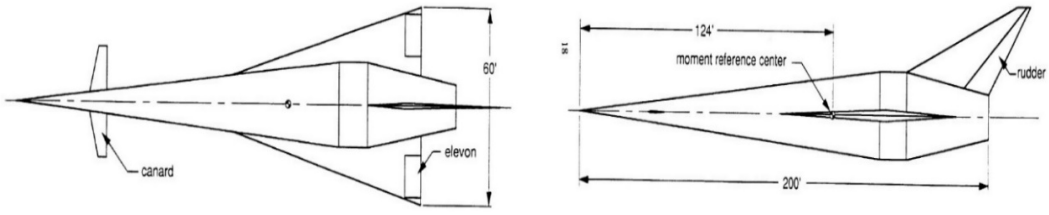

(a) (b)

Fig. 1 – GHV model [6] (a) top view (b) side view

Table 1 – Generic AHV Model Geometry Parameters

Notation	Parameter	Value
m	Mass	136080 Kg
S	Wing Reference Area	334.7295 m^2
b	Wing Span	18.2880 m
c	Mean Aerodynamic Chord	24.384 m
x_{mrc}	Moment Reference Centre	37.7952 m
g	Gravity	9.8 m/sec^2
T_{max}	Maximum Thrust	1467900 N
I_{sp}	Specific Impulse	1000 s

The translational dynamics and kinematic equations are given by,

$$\dot{u} = F_{ax}/m + F_{Tx}/m - qw - g\sin\theta \quad (1)$$

$$\dot{w} = F_{az}/m + uq + g\cos\theta \quad (2)$$

$$\dot{x} = u\cos\theta + w\sin\theta \quad (3)$$

$$\dot{z} = u\,sin\theta - w\,cos\theta \quad (4)$$

The rotational dynamics and kinematic equations are given by,

$$\dot{q} = M_z/I_{yy} \quad (5)$$

$$\dot{\theta} = q \quad (6)$$

3DOF AHV Longitudinal translational and rotational dynamics Equation (1-6) of the model can be transformed and modelled into the Equation (7-12) using the wind axis representation and are given by,

$$\dot{V} = (T\cos\alpha - \overline{q}SC_D - mg\sin\theta)/m \quad (7)$$

$$\dot{\gamma} = (T\sin\alpha + \overline{q}SC_L - mg\,cos\theta)/mV \quad (8)$$

$$\dot{q} = \overline{q}ScC_m/2I_{yy} \quad (9)$$

$$\dot{\theta} = q \quad (10)$$

$$\dot{R} = V\,cos\theta \quad (11)$$

$$\dot{h} = V\sin\gamma \quad (12)$$

Considering, $\alpha = \theta - \gamma$, and obtaining $\dot{\alpha}$, is given by the Equation (13).

$$\dot{\alpha} = q - (1/mV)(T\sin\alpha + \overline{q}SC_L - mg\cos\theta) \tag{13}$$

The AHV model using the Equation (7-13) are represented by the states described by $[V,\gamma,\alpha,\theta,q,h]'$ for the model simulation. The aerodynamics model for the winged-cone GHV model is used from [7], to achieve the aerodynamic coefficient C_L, C_D and C_m. These coefficients show variation with the Mach number, M and α for the complete flight regime, and includes the variation with different propulsion and engine models. MATLAB is used to create subroutines and interpolation for the model simulation. The lift force, drag force and pitching moment are expressed by $L = \overline{q}SC_L$, $D = \overline{q}SC_D$ and $M = \overline{q}cSC_m$ and the lift coefficient, drag coefficient and pitching moment coefficient are given by the Equation (14-16). These linear relations of aerodynamic coefficients given by Equation (14-16) are considered for the 3DOF longitudinal model simulation of AHV and are also used to implement the bifurcation method with the elevator deflection δ_e.

$$C_L = C_{L\alpha}.\alpha + C_{L\delta e}.\delta_e \tag{14}$$

$$C_D = C_{D\alpha}.\alpha + C_{D\delta e}.\delta_e \tag{15}$$

$$C_m = C_{m\alpha}.\alpha + C_{m\delta e}.\delta_e + C_{mq}.(q.c/2V) \tag{16}$$

The generic AHV vehicle uses the combined propulsion engine model with hypothetical proposed design engine model from [8], using the turbojet (T_{E1}), ramjet and scramjet (T_{E2}), and rocket (T_{E3}) for the complete AHV flight envelope. For the dynamic simulation of 3DOF AHV model, combined thrust models given by the Equation (17-20) is implemented. The thrust models represent the functional relation with the Pilot Lever Angle (PLA) or thrust factor, Mach number and altitude for the entire flight envelop.

Table 2 – Different propulsion models

Propulsion Engine	Engine	Mach No. Range
Turbojet Engine	E1	$0 < M \leq 2$
Ramjet and Scramjet Engine	E2	$2 < M \leq 6$
Rocket Engine	E3	$6 < M \leq 24$

$$T_{E1} = PLA\left(299000 - 10h + 0.000133h^2 - (6.48\cdot 10^{-10}\cdot h^3 + 3750M^3\right) \tag{17}$$

$$T_{E2} = PLA\begin{pmatrix} 753M^7 - 1500M^6 + 116000M^5 - 436000M^4 \\ +807000M^3 - 697000M^2 + 394000M + 3.93\cdot 10^{-8}\end{pmatrix} \tag{18}$$

$$\text{For } h < 57000,\quad T_{E3} = -54300 + 0.664h + 324000PLA + 0.374(h\cdot PLA) \tag{19}$$

$$\text{For } h > 57000\quad T_{E3} = -16400 + 324000h + 324000PLA + 21295PLA \tag{20}$$

When the altitude varies in response to the associated AHV model output as Mach number, an atmospheric model including temperature and air density is needed. Because the fluctuation in height affects the temperature and density of the atmosphere, the inverse relationship between the two from [9] is applied to the 3DOF AHV model simulation.

3. AERODYNAMIC MODEL ANALYSIS

The vehicle dynamics stability study provides a challenging behavior to develop a comprehensive interpretation of the broad flight envelope, particularly when the transition

takes place from subsonic speed to varying sonic velocities and to high hypersonic speeds. The pitching moment coefficient plays a significant part in the stability analysis of the longitudinal dynamics of the generic AHV and its variation with the Mach number, M for the different angle-of-attack, α is shown in Fig. 2 (a). For the static longitudinal stability of the vehicle, the value of C_m must be be negative, and the value of positive and negative C_m refer to nose up and nose down pitching moment respectively, C_m changes with the change of α. The aerodynamics incremental derivative C_{m_α} is obtained for the selected angle of attack, α for -1 and 4 degrees for the complete flight envelope varying the Mach number, M=0 to 24 and is shown in Fig. 2 (b).

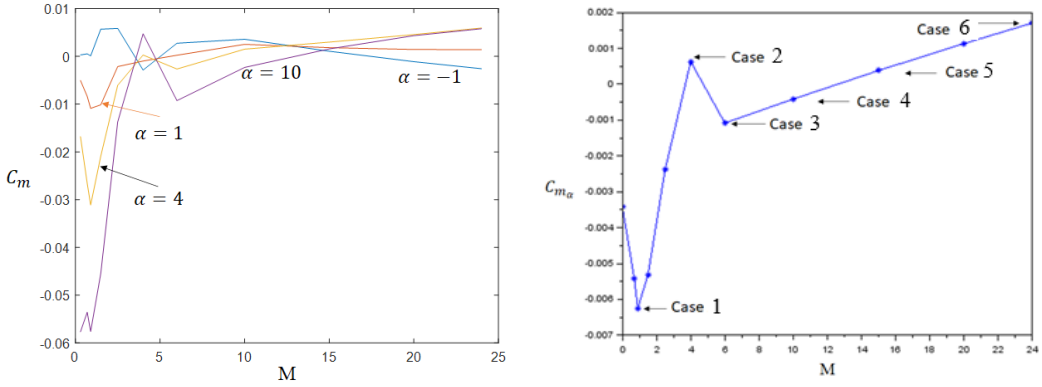

Fig. 2 – Aerodynamic coefficient (a) Pitching moment C_m with M (b) Incremental derivative C_{m_α}

Different cases of C_{m_α} are identified from Fig. 2 (b) for the entire flight envelope and are represented in Table 3. These cases represent the different AHV flight phases of ascent, descent and level corresponding to different Mach numbers. These cases are used for longitudinal trim analysis and trim simulation of the AHV for the complete flight envelope.

Table 3 – Different simulation cases for 3DOF AHV model

Cases	Mach Number (M)	Flight Phase
1	0.9	Ascent/Descent
2	4	Ascent/Descent
3	6	Ascent/Descent
4	10	Level
5	15	Level
6	24	Level

4. LONGITUDINAL TRIM ANALYSIS

The longitudinal nonlinear dynamic AHV model presented with Equation (7-13) is used to obtain the solution for the trim or equilibrium states. These states are V, γ, q, θ and α, in which the states V, γ and θ are considered to be zero, i.e., considering the model to be flying with constant V, γ and θ values. In this situation the flight is in a straight path with the possible conditions as γ=0 for the level flight, γ=positive value for the ascend flight or γ=negative value for the descending flight, and at the same time with the constraint that the nose orientation is constant i.e., θ=constant. To achieve these trim conditions for the AHV flight, we obtain the trim states by setting left-hand side of Equation (7-13) to zero and solving for the right-hand

side, and this is given by Equation (21-24).

$$0 = (T\cos\alpha - \overline{q}SC_D - mg\sin\theta)/m \tag{21}$$

$$0 = (T\sin\alpha + \overline{q}SC_L - mg\cos\theta)/mV \tag{22}$$

$$0 = \overline{q}ScC_m/2I_{yy} \tag{23}$$

$$q = 0 \tag{24}$$

The trim states are represented by (*) and are given by the following Equation (25-27).

$$C_D^* = (T^*\cos\alpha - mg\sin\theta)/\overline{q}^*S \tag{25}$$

$$C_L^* = (mg\cos\theta - T^*\sin\alpha)/\overline{q}^*S \tag{26}$$

$$C_m^* = 0 \tag{27}$$

In case of climbing condition of flight, from Equation (27) we obtain the climb angle and the climb rate respectively given by the following Equation (28-29).

$$\sin\gamma^* = \left(T^*\cos\alpha - \overline{q}^*SC_D^*\right)/mg \tag{28}$$

$$(\mathrm{V}\sin\gamma)^* = \left(T^*\cos\alpha - \overline{q}^*SC_D^*\right)V^*/mg \tag{29}$$

From Equation (25) we can write the thrust relation given by Equation (30).

$$T^* = \frac{\overline{q}^*SC_D^* + mg\sin\theta}{\cos\alpha} \tag{30}$$

The drag curves obtained using the trim analysis are shown in Fig. 3 with M and α variation and the trim states obtained are used for the AHV model dynamic simulation and using them as initial conditions or initial values for the simulation are also used as the initial values to implement the bifurcation method.

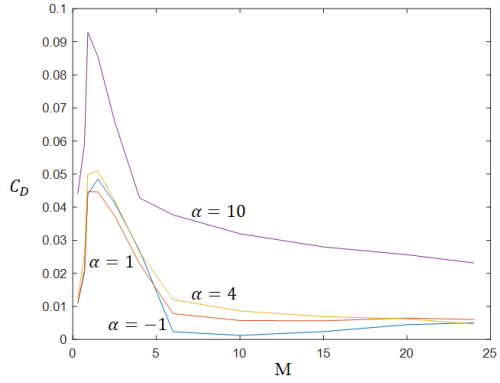

Fig. 3 – Aerodynamic coefficient C_D with M and α variation

5. AHV MODEL SIMULATION

Simulation of the 3DOF generic AHV longitudinal dynamic nonlinear model is carried out and the states V, γ, α, θ, q and h, are obtained at different Mach numbers and altitudes. Here, V is replaced by Mach number M and is obtained using $M=V/a$ where a is the speed of sound. The simulation is carried out for the trimmed states or at equilibrium points as discussed above. Here, V^* and h^* are considered constant values, $\gamma^*, \alpha^*, \theta^*$, $q=0$ and T^* are used from

Equation (17-20) depending upon the different Mach number range is considered for all different trim or equilibrium points, as for the simulation cases, shown in Table 4. The linear longitudinal AHV model is obtained considering Equation (7-13) and the state space representation is given by $\dot{x}=Ax+Bu$, where the state is represented as $x=[M, \gamma, \alpha, \theta, q, h]'$ and the input as u= [δe, PLA]. The dynamic 3DOF generic AHV longitudinal model simulation is carried out for the different cases outlined in Table 4 for different Mach numbers and the corresponding altitudes. The simulation is carried out for trim conditions considering the elevator deflection, δ_e as zero for all cases shown in Table 4; the magnitude of PLA is considered as an incremental value between 0.1 to 1 for all cases. The aerodynamic coefficient with their derivatives from Table 5 is used in the simulation for the different cases.

Table 4 – Different simulation cases for 3DOF generic AHV longitudinal model

Simulation Cases	Mach Number (M)	Altitude (h), ft
1	0.9	10,000
2	4	50,000
3	6	65,000
4	10	10,0000
5	15	10,0000
6	24	10,0000

Table 5 – Aerodynamic derivatives versus Mach

Mach No.	C_{L_α}	$C_{L_{\delta e}}$	C_{D_α}	$C_{D_{\delta e}}$	C_{m_α}	$C_{m_{\delta e}}$
0.9	0.0252	-0.0032	0.00005	0.00006	-0.0052	0.0024
4	0.0134	0.005	-0.0009	-0.0039	0.0007	0.0006
6	0.0147	-0.0006	0.0013	-0.0006	-0.0011	-0.000005
10	0.0132	0.001	0.0008	-0.0004	-0.0004	-0.0003
15	0.0115	0.0002	0.0002	-0.0005	0.0006	-0.00007
24	0.0072	-0.002	-0.0009	-0.0007	0.0022	0.0002

The dynamic 3DOF generic AHV longitudinal model simulation is carried out for the different cases outlined in Table 4. The simulation is carried out at six different Mach numbers and at corresponding altitudes. The simulation cases are shown in Fig. 4 to 9.

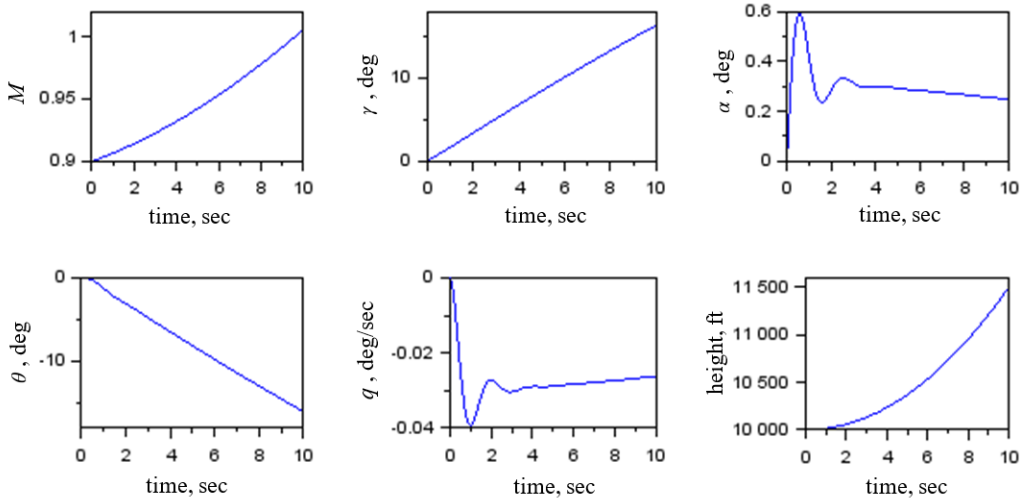

Fig. 4 – Dynamic Simulation Case 1 for M = 0.9

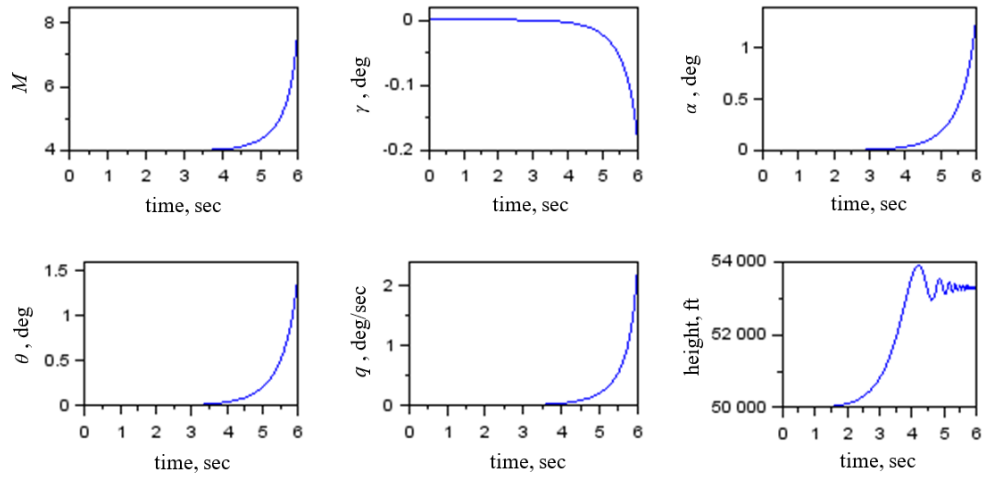

Fig. 5 – Dynamic Simulation Case 2 for M = 4

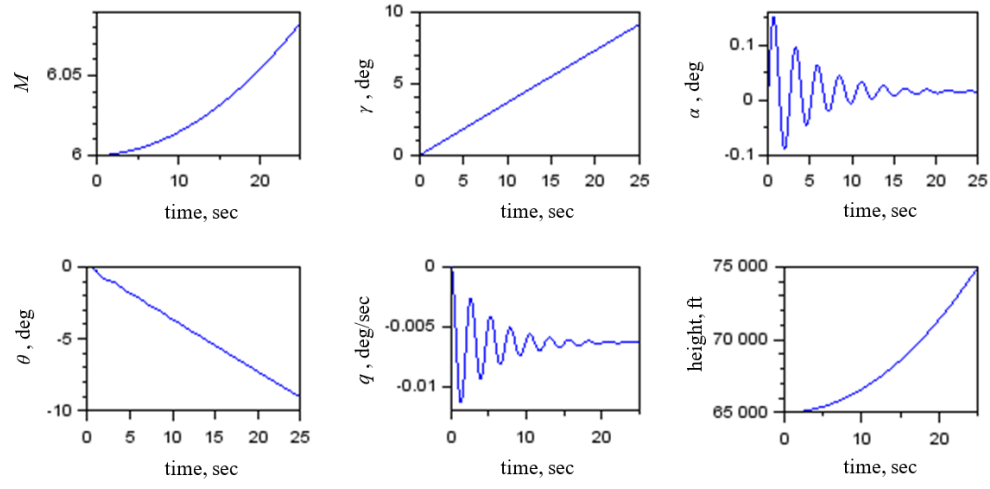

Fig. 6 – Dynamic Simulation Case 3 for M = 6

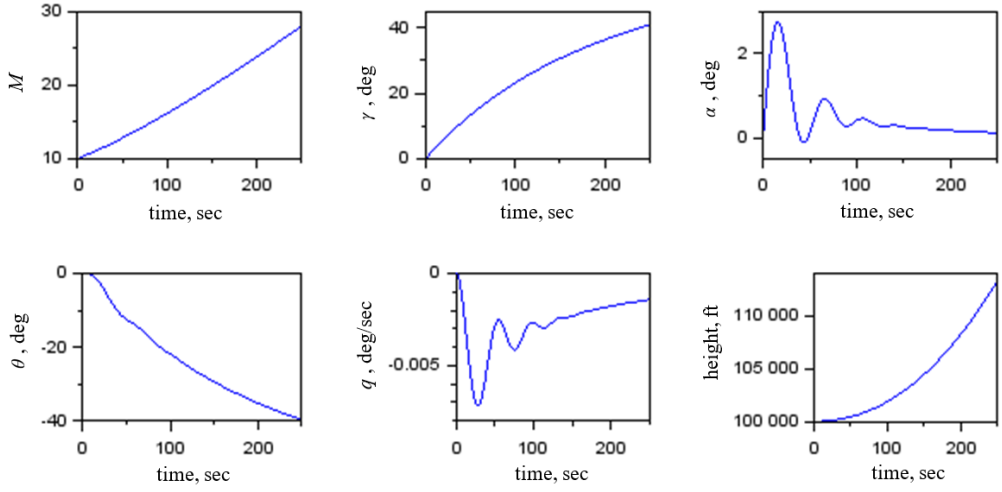

Fig. 7 – Dynamic Simulation Case 4 for M = 10

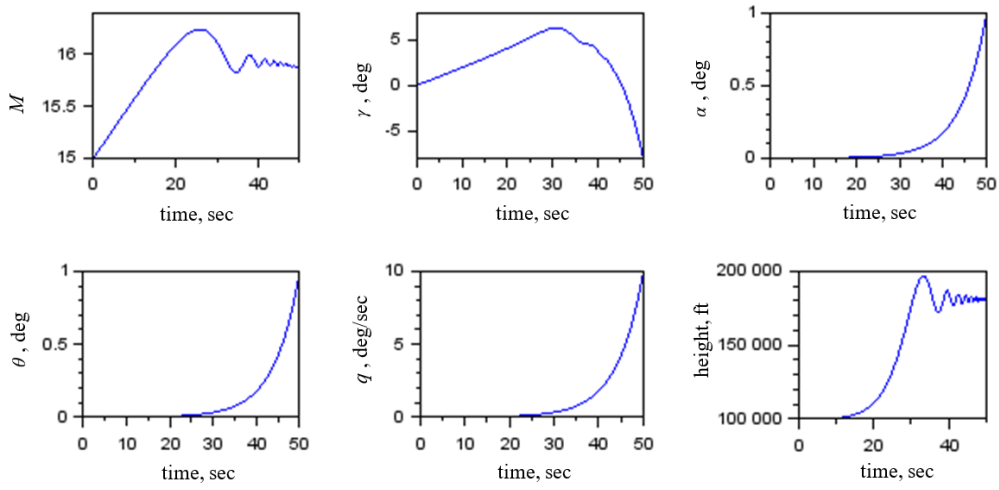

Fig. 8 – Dynamic Simulation Case 5 for M = 15

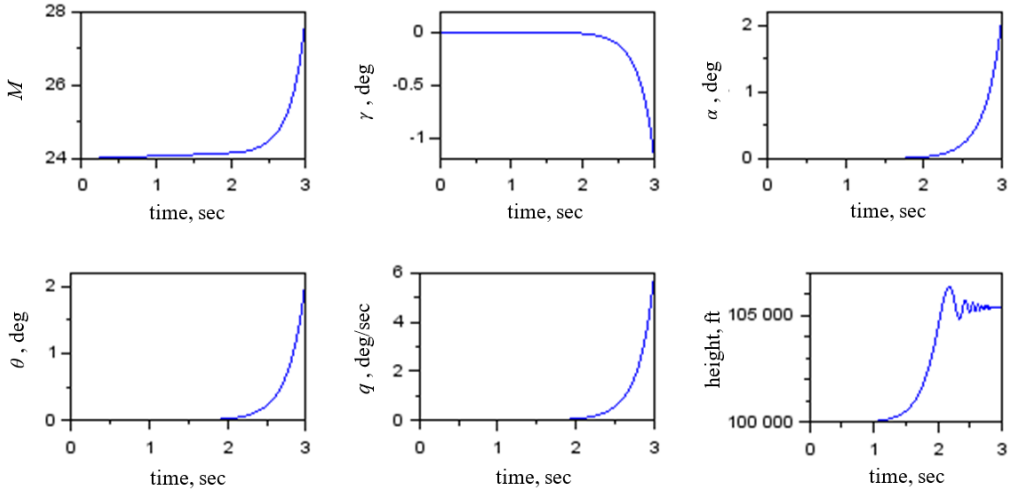

Fig. 9 – Dynamic Simulation Case 6 for M = 24

5.1 Dynamic Stability Analysis

The dynamic stability analysis of the AHV model at different Mach number is performed. Case 1 simulation shown in Fig. 4, shows that the angle of attack, α is stabilizing near α=0.25 degrees with the increase in the AHV speed for Mach number, M=0.9, and with the gain in height. The pitch rate, q is stabilizing near q=0.035. The overall dynamic simulation for the case shows the stable short period dynamic behavior and the angle of attack, α shows converging nature, near the equilibrium or trim point. Some more simulation time will show long period dynamic behavior. Case 2 simulation shown in Fig. 5, shows that the angle of attack, α shows breakdown behavior near α=5 degrees with the increase in the AHV speed for Mach number, M=4, and with the gain in altitude, and then shows a constant behavior in height. The flight path angle, gamma maintains the flight of γ=-0.2 degrees and increase in nature, and the pitch rate, q also shows a breakdown behavior. The overall dynamic trim simulation for the case shows an unstable behavior and the angle of attack, α shows a divergence nature, near to the equilibrium or trim point.

Case 3 simulation shown in Fig. 6, shows that the angle of attack, α is stabilizing near

α=0.03 degrees with the increase in the AHV speed for Mach number, M=6, and with height gain. The flight path angle, γ increases from γ=0 to 10 degrees and the pitch rate, q is stabilized near q=0.005. The overall dynamic simulation for the case shows the stable behavior and the angle of attack, α shows the convergent nature, near to the equilibrium or trim point. Case 4 simulation shown in Fig. 7, shows that the angle of attack, α is stabilizing near α=0.02 degrees with the increasing AHV speed for Mach number, M=10, and with height gain. The flight path angle, γ maintains the flight and the pitch rate, q is maintained near to q=0.002. The overall dynamic simulation for the case shows the stable behavior and the angle of attack, α shows convergent nature, near the equilibrium or trim point.

Case 5 simulation shown in Fig. 8, shows that the angle of attack, α has breakdown behavior near α=0.5 degrees with the increase in the AHV speed for Mach number, M=15, and with the gain in altitude, and then shows constant and level flight behavior in height. The flight path angle, γ maintains the flight of γ=5 degrees and flight of γ=-5 degrees and greater is observed, and the pitch rate, q also shows breakdown behavior. The overall dynamic simulation for the case shows unstable behavior and the angle of attack, α shows divergence nature, near to the equilibrium or trim point. Case 6 simulation shown in Fig. 9, shows that the angle of attack, α shows breakdown behavior near α=1 degrees with the increase in the AHV speed for Mach number, M=24, and with the gain in altitude, and then shows constant and level flight behavior in height. The flight path angle, γ maintains the negative heading to γ=-0.5 degrees is observed, and the pitch rate, q also shows breakdown behavior. The overall dynamic trim simulation for the case shows unstable behavior and the angle of attack, α shows divergence nature, near to the equilibrium or trim point. The dynamic stability for all different simulation cases and Mach number is shown in Table 6.

Table 6 – Dynamic stability for the simulation cases

Simulation Cases	Mach Number (M)	Stability
1	0.9	Stable
2	4	Unstable
3	6	Stable
4	10	Stable
5	15	Unstable
6	24	Unstable

5.2 Bifurcation Method Analysis

The Bifurcation Method provides a possibility to enhance vehicle control design parameters by using the bifurcation approach to exhibit global stability. The method provides quantitative information on global stability and offers strategies to stabilize the nonlinear behavior of the aircraft. The Method uses a Continuation Based Algorithm (CBA) to study the nonlinear dynamical models using ordinary differential equations (ODE) of the first order and determines the steady states and different equilibrium points, by using the software AUTO-07p [10]. ODE are represented as a function of states variables and control parameters given by, $\dot{x}=f(x,u)$, the solution of the nonlinear equation is determined by, $\dot{x}=f(x,u,p)=0$, by keeping the constraint p fixed with varying next parameter u, and this results in the finding of all trim states. The Standard Bifurcation Analysis (SBA) method is implemented with CBA. In this approach, the continuation algorithm computes all solutions with trim states of the system considering the varying and fixed parameters and also determines the details of local stability at every trim state. The changes in the branch stability of the trim states solution are called or represented by the 'Bifurcation Points'. These 'Bifurcation Points' indicate the

moment of the Eigenvalues leading to an unstable system in the stability plane i.e., the movement of the system Eigenvalues migrates from the left half to the right half of the complex plane, and prominently shows the unstable dynamical system occurrence or behavior.

The method is implemented for the 3DOF longitudinal AHV model by applying SBA for the nonlinear dynamic model [11]. The dynamic model represented for the 3DOF AHV model simulation is used for the method implementation [12], and the state variables are given by x=[M,γ,α,θ,q,h]′. The states are further reduced for simplicity, considering constant Mach number, M, constant height, h and considering very small changes in γ, thus the state variable considered for the analysis is reduced and is given by x=[α,θ,q]′. The SBA for the AHV is implemented and bifurcation diagram with Eigen values for each case is obtained which shows the flight dynamics behaviour. The bifurcation diagram for M=0.9 is shown in Fig. 10. The stability information can be examined for the longitudinal dynamic model using Eigenvalues obtained from the bifurcation analysis. The system behaviour might be stable or unstable depending on these Eigenvalues. The different Eigenvalues obtained using the bifurcation method for the different cases with Mach number is shown in Table 7. The Eigenvalues obtained are used to plot the pole-zero map to understand the system stability behaviour and are shown in the Fig. 11. The poles plot for the different simulation cases shows that Cases 1, 3 and 4 show stable behaviour and Cases 2, 5 and 6 show unstable behaviour due to the poles lying on the RHS plane.

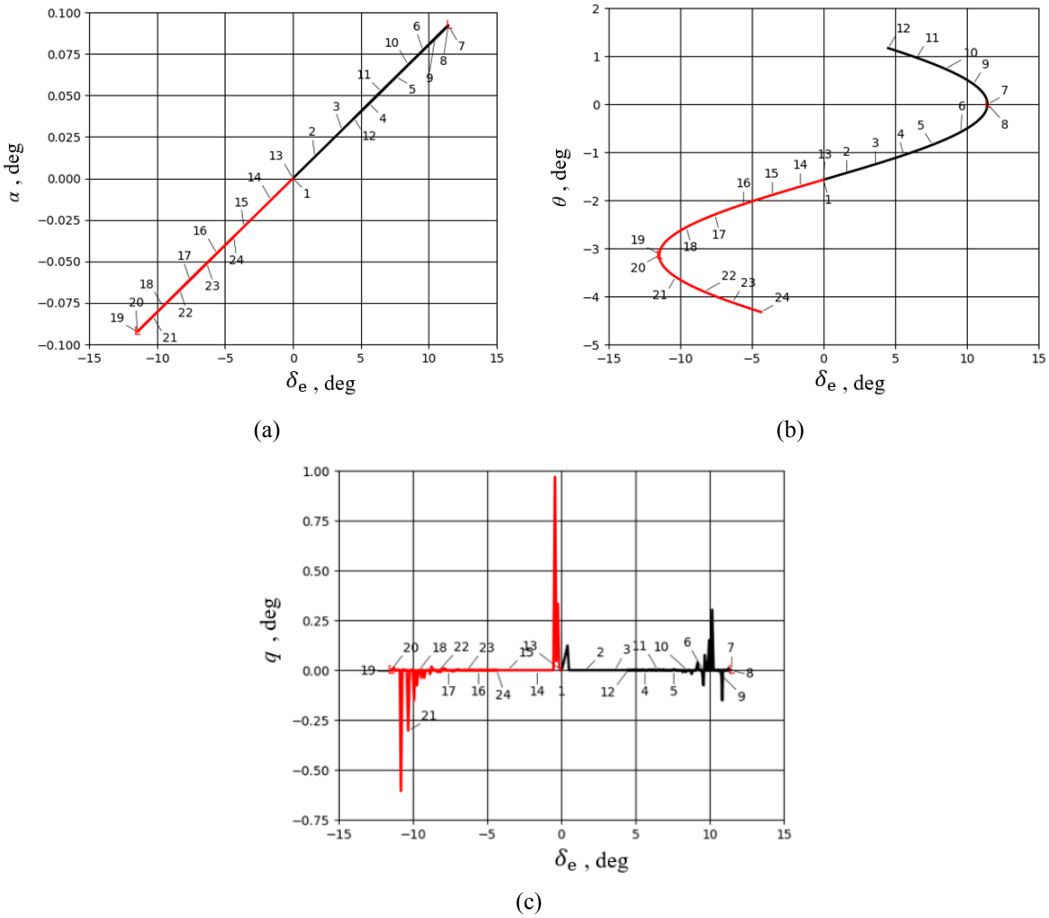

Fig. 10 – Bifurcation Diagram (a) α (b) θ (c) q

Table 7 – Eigen values obtained using Bifurcation Method

Simulation Cases	Mach Number (M)	Eigenvalues	Stability
1	0.9	-0.0305831, -1.192±j3.123	Stable
2	4	1.69283, -0.009158, -2.49717	Unstable
3	6	-0.006419, -0.021±j2.501	Stable
4	10	-0.00523866, -0.0086±j0.073	Stable
5	15	0.123599, -0.003423, -0.150586	Unstable
6	24	3.11523, -0.002149, -3.19905	Unstable

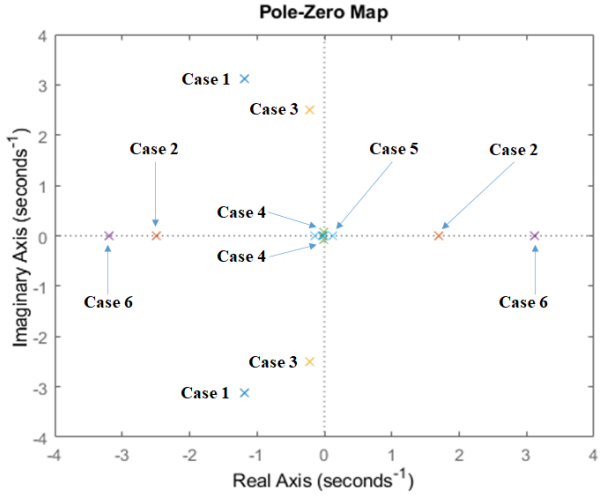

Fig. 11 – System Poles plot for the simulation cases

The corresponding longitudinal modes for simulation cases 1, 3 and 4 are obtained and are shown in Table 8.

For cases 1 and 4 at Mach number M=0.9 and M=10 it shows short period behavior for the AHV flight, and for case 3 at Mach number M=6 it shows long period or phugoid behavior for the AHV flight.

Cases 2, 5 and 6 at Mach number M=4, M=15 and M=24 indicates unstable or instability behavior for the AHV flight.

This unstable Mach number for the AHV flight can be made stable with the design of suitable control design methods, and hence the entire flight envelope of the AHV from Mach number M=0 to 24 can have a stable flight.

Table 8 – Simulation cases with longitudinal modes

Cases	Mach Number	Frequency (rad/sec)	Damping Ratio	Periods (sec)	Numbers of cycles to damp to half amplitude of the respective modes
1	0.9	0.35665	0.3817	17.6081	2.8506, short period
2	4	-	-	-	-
3	6	0.00846	0.0084	742.2356	128.6150, long period
4	10	0.11803	0.1188	53.2044	9.1551, short period
5	15	-	-	-	-
6	24	-	-	-	-

6. CONCLUSIONS

The study presents the longitudinal trim with stability assessment of the 3DOF longitudinal AHV model with dynamic simulation and stability analysis using the bifurcation method. Trim analysis and simulation of the 3DOF AHV model are performed under the different cases of aerodynamic model analysis of incremental pitching coefficient for the corresponding Mach numbers. For the different 6 cases, trim simulation is performed with the AHV model resulting in the stable simulation for cases 1, 3 and 4 for Mach number M=0.9, M=6 and M=10, and for cases 2, 5 and 6 for Mach number M=4, M=15 and M=24 show unstable behavior. The validation of the cases is carried out with the bifurcation method implementation using the 3DOF AHV model with constant velocity. Using the bifurcation method, for all the different cases, the eigenvalues are obtained and corresponding poles are determined, and this shows and confirms the same findings for stable cases 1, 3 and 4 and unstable cases 2, 5 and 6. The longitudinal modes of the AHV show that cases 1 and 4 show a short-period behavior and case 3 shows a long-period or a phugoid behavior. The bifurcation analysis results presented here demonstrate a potential way for determining the stability of different trim points.

REFERENCES

[1] A. D. Marco, E. L. Duke and J. S. Berndt, *A General Solution to the Aircraft Trim Problem*, AIAA Modeling and Simulation Technologies Conference and Exhibit, Hilton Head, South Carolina, US, August 20-23, AIAA, 2007.

[2] O. Prakash, A. Daftary and N. Ananthkrishnan, *Trim and Stability Analysis of Parafoil/Payload System using Bifurcation Methods*, 18th AIAA Aerodynamic Decelerator Systems Technology Conference and Seminar, Munich, Germany, May 23-26, AIAA, 2005.

[3] G. Miller, D. Jacques and M. Pachter, *Aircraft Trim Control*, AIAA Guidance, Navigation, and Control Conference and Exhibit, Austin, Texas, Aug 11-14, AIAA, 2003.

[4] B. Chudoba and M. V. Cook, *Trim Equations of Motion For Aircraft Design: Steady State Straight-Line Flight*, AIAA Atmospheric Flight Mechanics Conference and Exhibit, Austin, Texas, Aug 11-14, AIAA, 2003.

[5] B. Chudoba and M. V. Cook, *Trim Equations of Motion For Aircraft Design: Turning Flight, Pull-Up and Push-Over*, AIAA Atmospheric Flight Mechanics Conference and Exhibit, Austin, Texas, Aug 11-14, AIAA, 2003.

[6] J. D. Shaughnessy, S. Z. Pinckney, J. D. Mcminn, C. I. Cruz and M. L. Kelley, *Hypersonic vehicle simulation model: Winged-cone configuration*, NASA Langley Research Center, NASA-TM-102610, United States, 1990.

[7] S. Keshmiri, R. Colgren and M. Mirmirani, *Development of an Aerodynamic Database for a Generic Hypersonic Air Vehicle*, AIAA Guidance, Navigation, and Control Conference and Exhibit, San Francisco, California, Aug 15-18, AIAA, 2005.

[8] S. Keshmiri, R. Colgren and M. Mirmirani, *Six-DOF Modeling and Simulation of a Generic Hypersonic Vehicle for Control and Navigation Purposes*, AIAA Guidance, Navigation, and Control Conference and Exhibit, Keystone, Colorado, Aug 21-24, AIAA, 2006.

[9] J. Roskam and C. T. Lan, *Airplane Aerodynamics and Performance*, Lawrence, Kansas. Darcorporation, Revised ed., 2000.

[10] E. J. Doedel, A. R. Champneys, T. F. Fairgrieve, Y. A. Kuznetsov, B. Sandstede, and X. Xang, *AUTO-07p: Continuation and Bifurcation Software for Ordinary Differential Equations*, Ver. AUTO-07p 2007, Department of Computer Science, Concordia University, Montreal, Canada, 2007.

[11] O. Prakash, R. Singh, S. Joshi and Y. Jeppu, *Flight Dynamics Analysis using High Altitude & Mach Number for Generic Air-Breathing Hypersonic Vehicle*, AIAA Propulsion and Energy Forum, Virtual Event, Aug 9-11, AIAA, 2021.

[12] N. K. Sinha and N. Ananthkrishnan, *Elementry Flight Dynamics with an Introduction to Bifurcation and Continuation Methods*, FL, USA, CRC Press, 2014.